Monte Carlo studies of the dynamics of an interacting monodispersive magnetic-particle system

J.-O. Andersson
Nordita, Blegdamsvej 17, DK-2100 Copenhagen Ø, Denmark

C. Djurberg, T. Jonsson, P. Svedlindh, and P. Nordblad
Department of Materials Science, Uppsala University, Box 534, S-75121 Uppsala, Sweden
(Received 7 July 1997)

The influence of the dipole-dipole interaction on the dynamics of monodispersive ensembles of magnetic nanoparticles have been studied by Monte Carlo simulations. An increased interaction strength drives the system from a state with only individual particle relaxation at all temperatures to a state where collective phenomena govern the dynamics at low temperatures. The collective nature of the dynamics is reflected in the appearance of magnetic ageing and a dramatically broadened relaxation function. [S0163-1829(97)06145-6]

I. INTRODUCTION

An ensemble of single domain magnetic particles forms a superparamagnetic state at high temperature. On lowering the temperature the particles become blocked at specific temperatures which depend on the size and magnetic anisotropy of the particles and the time scale of the experiment.[1] Depending on the size distribution of the particles, the macroscopic blocking temperature appears as a more or less sharp maximum in the ac susceptibility. If the concentration of particles is high, the dipole-dipole interaction affects the dynamics of the system. A concentrated ferrofluid offers a system where the dipole-dipole interaction strength can be continuously tuned by changing the particle concentration. Experiments on such systems show that the low-temperature dynamics is dramatically altered with increasing interaction strength. The blocking temperature on time scales of the order of seconds increases,[2] the maximum in the in-phase component of the ac susceptibility is broadened, and the frequency dependence of the out-of phase component is strikingly flattened at lower temperatures.[3] Additionally a spin-glass-like ageing phenomenon appears in the relaxation of the magnetization.[3–5] These results show that an increased interaction strength drives the system from a state where the dynamics is governed only by individual particle relaxation at all temperatures to a state where collective phenomena dominate the dynamics at low temperatures.

The random and competing interparticle interactions existing in a concentrated system may influence the dynamic properties in two different ways: (i) by affecting the barrier heights and hence the relaxation time of the individual particles and (ii) by giving rise to a collective behavior. One of the problems when trying to interpret the dynamic behavior of interacting particle systems is to determine whether one only observes the dynamic behavior of individually relaxing particles or if also dynamics governed by collective behavior is present.

The interpretation of results from experiments on ferrofluids is somewhat complicated by the inevitable particle size distribution that any real particle system is associated with. In this paper we use Monte Carlo (MC) simulations to investigate ensembles consisting of monodispersive magnetic particles of different concentrations. We have chosen to study monodispersive ensembles, in order to be able to most easily distinguish between collective dynamics and individual particle relaxation. It is found that strongly interacting systems give rise to collective dynamic behavior, manifested in the appearance of an ageing behavior and an ac susceptibility distinctly different from that of the noninteracting system.

In Sec. II, a description of the model and the methods is presented together with the details of the simulation, and in Sec. III, the ac susceptibility and magnetic relaxation results are presented and discussed.

II. MODEL AND METHOD

The model describes a magnetic system consisting of N magnetic particles with random but not overlapping positions and with the anisotropy axes distributed in random directions. The magnetic particles are placed in a cubic box with periodic boundary conditions. The particles are assumed to be spherical and monodispersive, i.e., having one single-particle radius r.

We use a standard Monte Carlo method for dynamical systems,[6] which has been shown to exhibit good qualitative agreement with experimental results when applied to spin glasses[7] and which now is adapted to this problem. Our description of a particle in the dipolar fields from the surrounding particles and in an external field follows a description developed by Chantrell *et al.*[8]

Defining $\hat{\mu}_i$ to be a unit vector along the direction of the magnetic moment $\vec{\mu}_i$ of particle i, i.e., $\vec{\mu}_i = M_s V_i \hat{\mu}_i$, and $\hat{n}_i$ a unit vector along the easy magnetization axis, the energy of particle i can be written

$$E_i = -KV_i(\hat{\mu}_i \cdot \hat{n}_i)^2 - M_s V_i \hat{\mu}_i \cdot \vec{B}_i, \tag{2.1}$$

where K is the anisotropy constant, V_i is the particle volume, and M_s is the saturation magnetization. The field $\vec{B}_i$ is the sum of the applied field and the dipolar fields from the surrounding particles,

$$\vec{B}_i = \mu_0 H_a \hat{z} + \frac{\mu_0}{4\pi} M_s \sum_{j \neq i} V_j \left[\frac{3(\hat{\mu}_j \cdot \vec{r}_{ij})\vec{r}_{ij}}{r_{ij}^5} - \frac{\hat{\mu}_j}{r_{ij}^3} \right], \tag{2.2}$$

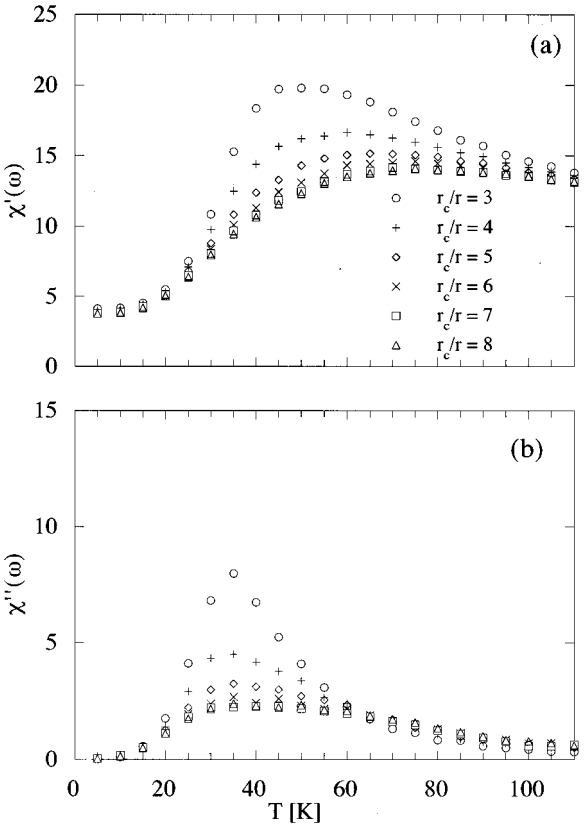

FIG. 1. The cutoff radius dependence of the ac susceptibility $\chi=\chi'-i\chi''$ for $r_c/r=3.0$, 4.0, 5.0, 6.0, 7.0, and 8.0. $\epsilon=7\%$, $f=1/1024$ (mcs)$^{-1}$, $N_{\rm mc}=16\,384$ mcs and $N_{\rm tr}=10$. (a) χ' and (b) χ''.

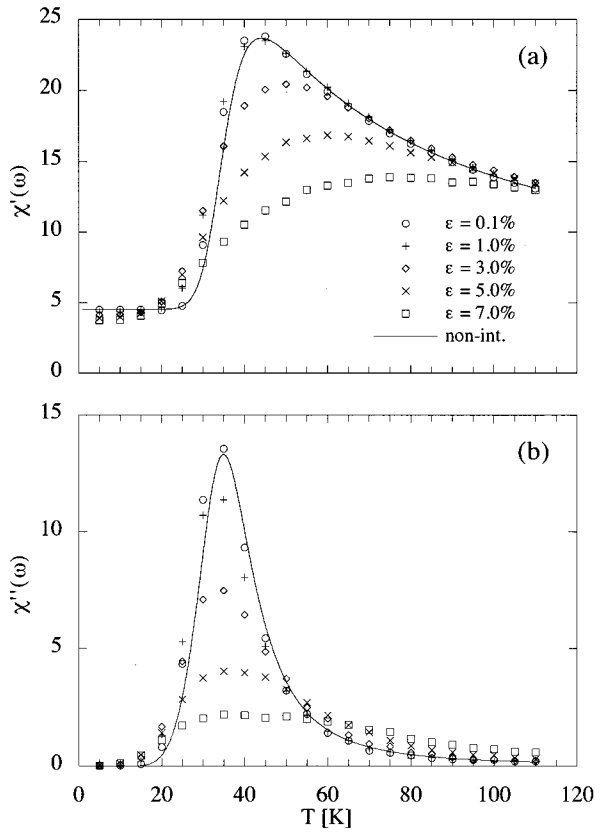

FIG. 2. The concentration dependence of the ac susceptibility $\chi=\chi'-i\chi''$ for $\epsilon=0.1$, 1.0, 3.0, 5.0, and 7.0. $f=1/1024$ (mcs)$^{-1}$, $N_{\rm mc}=16\,384$ mcs and $N_{\rm tr}=10$. The solid lines are the calculated results for a noninteracting system. (a) χ' and (b) χ''.

where $\vec{r}_{ij}$ is a vector connecting the magnetic moments i and j, $\vec{r}_{ij}=\vec{r}_i-\vec{r}_j$, and $r_{ij}=|\vec{r}_{ij}|$. The potential energy is thus a function of the direction of the magnetic moment $\hat{\mu}_i$, the easy axis $\hat{n}_i$, and the field $\vec{B}_i$. If the angle between $\hat{n}_i$ and $\hat{\mu}_i$ is denoted α_i and the angle between $\vec{B}_i$ and $\hat{\mu}_i$ denoted ρ_i, the expression for the energy can be written as

$$E_i=-KV_i\cos^2(\alpha_i)-M_sV_i|\vec{B}_i|\cos(\rho_i). \tag{2.3}$$

It can be shown that the minimum energy is found when all three vectors, $\hat{n}_i$, $\vec{B}_i$, and $\hat{\mu}_i$, lie in the same plane. In this case $\rho_i=\psi_i-\alpha_i$, where ψ_i is the angle between $\vec{B}_i$ and $\hat{n}_i$, and the energy can be expressed as

$$E_i=-KV_i[\cos^2(\alpha_i)+(M_s/K)|\vec{B}_i|\cos(\psi_i-\alpha_i)]. \tag{2.4}$$

The two minima and the saddle point of the energy are found using the Newton-Raphson technique. We require that the magnetic moment of a particle always stays in the direction of one of the two energy minima. The ''flipping'' probabilities for going between two minima are $p_i^1=\exp[-(E_i^s-E_i^1)/(k_BT)]$ and $p_i^2=\exp[-(E_i^s-E_i^2)/(k_BT)]$, respectively, where E_i^1 and E_i^2 are the energies of the two energy minima and E_i^s is the saddle-point energy. In order to update the direction of a moment, a unit vector perpendicular to $\hat{n}_i$ in the plane of $\hat{n}_i$ and $\vec{B}_i$ is found, $\hat{q}_i=[\vec{B}_i-(\hat{n}_i\cdot\vec{B}_i)\hat{n}_i]/|\vec{B}_i-(\hat{n}_i\cdot\vec{B}_i)\hat{n}_i|$. Since the new direction of the magnetic moment should be in the same plane with an angle α_i to $\hat{n}_i$, it is given by $\hat{\mu}_i=\hat{n}_i\cos(\alpha_i)+\hat{q}_i\sin(\alpha_i)$.

The transition rates between the two minima are given by $\nu_i^1=\tau_0^{-1}p_i^1$ and $\nu_i^2=\tau_0^{-1}p_i^2$, respectively, where τ_0 is a microscopic flip time. The unit of time in our simulation is one Monte Carlo Sweep (mcs), which corresponds to updating all particles in the system one after the other. This implies that τ_0, which for an experimental system is of the order 10^{-9}–10^{-11} s, corresponds to 1 mcs in the simulations.

Although in reality every particle interacts with every other particle, to include all interactions in the computation would be unnecessary and time consuming. Therefore the sum in Eq. (2.2) is truncated, only including neighbors within a cutoff radius r_c, i.e., particles i and j are included if $r_{ij}<r_c$.

We perform two kinds of dynamical simulations, ac susceptibility and zero-field-cooled (ZFC) relaxation simulations. In the ac simulations, the applied field varies as $H_{\rm ac}\sin(\omega t)\hat{z}$. The ac susceptibility $\chi=\chi'-i\chi''$ can then be calculated as

$$\chi'=\frac{2}{N_{\rm mc}H_{\rm ac}}\sum_{t=1}^{N_{\rm mc}}m(t)\sin(\omega t), \tag{2.5}$$

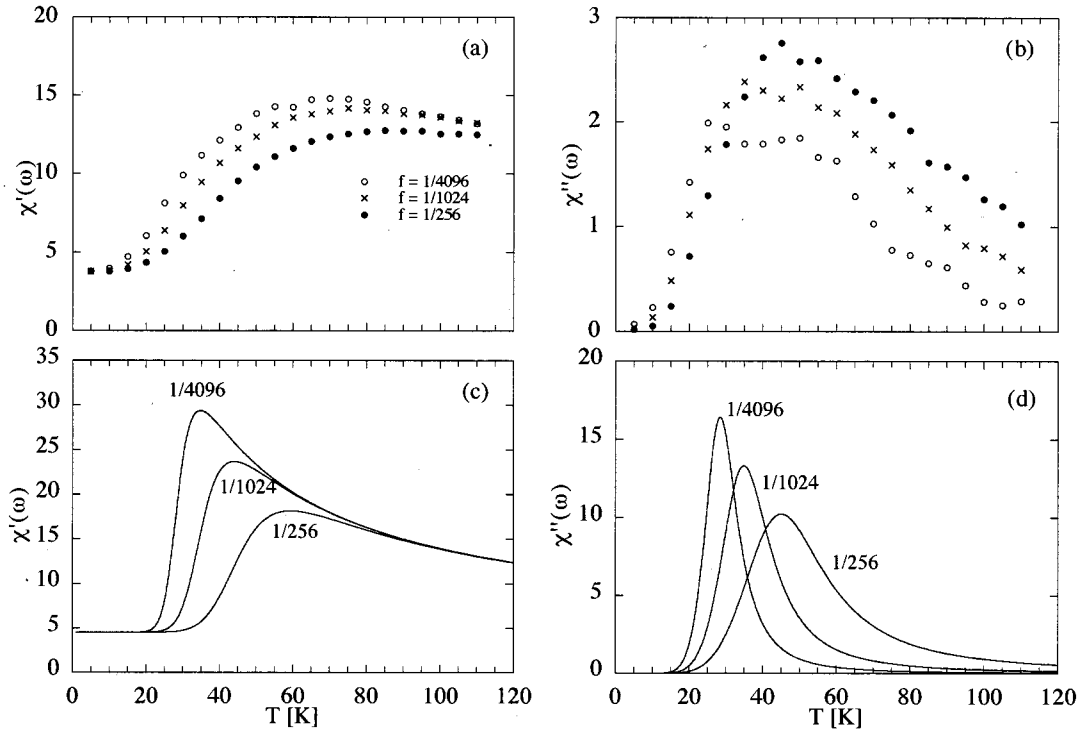

FIG. 3. Frequency dependence of the ac susceptibility $\chi=\chi'-i\chi''$ for $f=1/256$, 1/1024, and 1/4096 $(\mathrm{mcs})^{-1}$. (a) χ' and (b) χ'' for the interacting system. $\epsilon=7\%$, $N_{\mathrm{mc}}=16\,384$ mcs and $N_{\mathrm{tr}}=10$. (c) χ' and (d) χ'' for the noninteracting system.

$$\chi''=-\frac{2}{N_{\mathrm{mc}}H_{\mathrm{ac}}}\sum_{t=1}^{N_{\mathrm{mc}}}m(t)\cos(\omega t), \tag{2.6}$$

where $m(t)=M_s\Sigma_{i=1}^{N}V_i\langle\hat{\mu}_i(t)\cdot\hat{z}\rangle/\Sigma_{i=1}^{N}V_i$ is the magnetization due to the ac field. It should be noted that for this to make sense, $N_{\mathrm{mc}}f$ has to be an integer, where $f=\omega/2\pi$ is the frequency.

In the ZFC simulations the system is quenched in zero field to a relatively low temperature T, followed by an equilibration of the particle system for a time t_w. After the equilibration, a weak magnetic field h is applied and the magnetization $m_{\pm}(t)$, for both positive and negative h is studied as a function of time t (measured in mcs). The magnetization $m_{\pm}(t)$ is then used to calculate the susceptibility according to $\chi(t)=[m_+(t)-m_-(t)]/2h$. The results at each mcs are used to get average values at logarithmically spaced times.

In our model, the directions of the particle magnetic moment corresponding to the two energy minima are shifted towards the direction of the applied field as soon as the field is applied. This gives rise to a net magnetization (even when no flips have occurred), which leads to a temperature-independent nonzero contribution to the susceptibility. The results of calculations for the noninteracting case, shown in the Appendix, are

$$\chi(t)=\frac{M_s^2}{3K}\left[1+\frac{KV}{k_BT}(1-e^{-t/\tau})\right]. \tag{2.7}$$

for the ZFC susceptibility and

$$\chi'(\omega)=\frac{M_s^2}{3K}\left[1+\frac{KV}{k_BT}\frac{1}{1+(\omega\tau)^2}\right], \tag{2.8}$$

$$\chi''(\omega)=\frac{M_s^2}{3}\frac{V}{k_BT}\frac{\omega\tau}{1+(\omega\tau)^2} \tag{2.9}$$

for the ac susceptibility.

Since we are interested in zero-field dynamics, care has to be taken to ensure that H_{ac} and h are small enough for a linear response but large enough to give as good an accuracy as possible of the calculated quantity. We have found $H_{\mathrm{ac}}=240$ A/m and $h=240$ A/m to be appropriate choices.

The simulation procedure is repeated for N_{tr} statistically independent trajectories using different initial conditions, i.e., different particle positions, easy axes and initial particle magnetization directions, for each trajectory. The value of N_{tr} used in the different runs is given in the figure captions. The number of particles in the system is $N=1000$ in all cases. In all our simulations, the saturation magnetization is set to $M_s=4.2\times10^5$ A/m and the anisotropy constant used is $K=1.6\times10^4$ J/m^3, values that are similar to those of the γ-Fe_2O_3 particles studied in Ref. 9. The particle radius was chosen to be $r=3.5$ nm. The ac and ZFC susceptibility results presented below are given in SI units.

III. RESULTS AND DISCUSSION

As was mentioned in Sec. II, it is necessary to limit the range of the dipole-dipole interactions in the simulations. It is not *a priori* known where to put the cutoff. We have simply chosen to use the value of r_c where, within the statistical accuracy of the simulation, a further increase of r_c

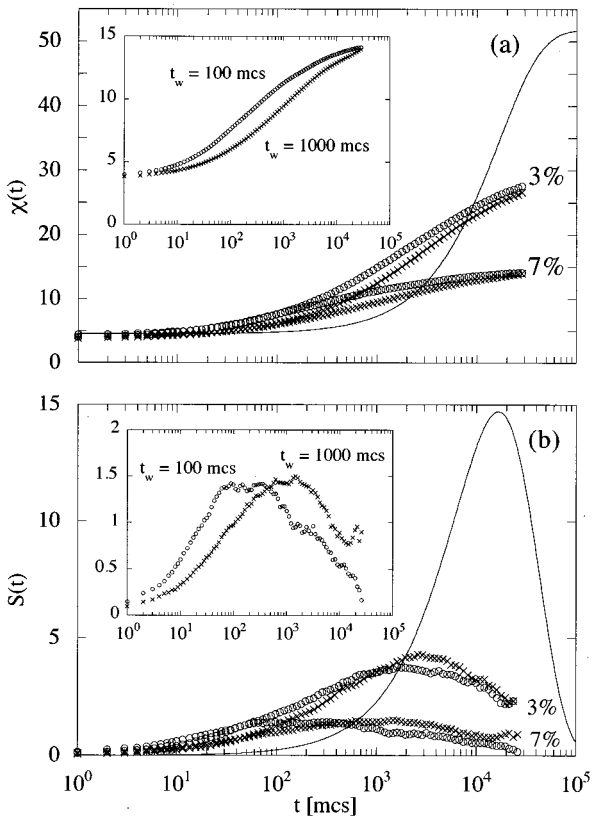

FIG. 4. ZFC relaxation for $\epsilon = 3\%$ and 7% and $t_w = 100$ and 1000 mcs. The calculated relaxation and relaxation rate curves for the noninteracting system are also shown. $T = 20$ K, $N_{\mathrm{tr}} = 200$. (a) $\chi(t)$, (b) $S(t) = \partial\chi(t)/\partial \ln(t)$. The insets show the behavior of the 7% sample in an enlarged scale.

does not change the results. In Fig. 1 the ac susceptibility is plotted for increasing cutoff radius for the highest (7%) concentration. A strong dependence on r_c is seen for the lower r_c values ($r_c/r = 3$, 4, and 5). For $r_c/r \geq 8$ there is no measurable change of the susceptibility. The same limiting value $r_c/r = 8$ was found to apply also for the systems with lower particle concentration.

The complex ac susceptibility, $\chi = \chi' - i\chi''$, has experimentally been shown to be a property sensitive to the dipole-dipole interparticle interaction.[3,5,10] In Fig. 2 the in-phase (a) and the out-of-phase (b) components of the susceptibility at a frequency of 1/1024 $(\mathrm{mcs})^{-1}$ are plotted versus temperature for particle concentrations (ϵ) ranging from 0.1 to 7%. The susceptibility shows a remarkable concentration dependence, manifested by a substantial suppression of the magnitude as well as a broadening of the maxima in both components. At low temperatures the in-phase component approaches a constant nonzero value intrinsic to the model as discussed above.

The ac susceptibility of the two most diluted systems, 0.1 and 1%, almost coincide with the analytically calculated curve (solid lines in Fig. 2). This indicates that these two-particle systems, at the time scales and temperatures considered, may be regarded as essentially noninteracting ensembles.

In a noninteracting system the dynamics is well described by an ensemble of individually relaxing particles.[3,9,11,12] The strongly interacting case is more complex. In Fig. 3, the in-phase (a) and the out-of-phase (b) components for the most concentrated system, 7%, are plotted versus temperature for three different frequencies, 1/256, 1/1024, and 1/4096 $(\mathrm{mcs})^{-1}$. In Figs. 3(c) and 3(d), the analytically calculated in-phase and out-of-phase components of the susceptibility for a noninteracting system at the same frequencies are plotted. Comparing the susceptibility of the strongly interacting system to that of the noninteracting ensemble striking differences are evident: a strong suppression and broadening of the maxima in the out-of-phase component, a less pronounced frequency dependence of the maxima in both susceptibility components and a shift of the maxima in the susceptibility towards higher temperatures. At temperatures above 80 K for the displayed frequencies, the in-phase component of the noninteracting system is essentially frequency independent and decays with temperature according to a modified Curie law. The interacting system shows a frequency dependence of χ' up to higher temperatures than the noninteracting system and consequently also the out-of-phase component sustains to higher temperatures. It is also noticeable that at temperatures below the maxima in the out-of-phase component of the interacting system $\chi''(\omega,T)$ becomes almost frequency independent whereas $\chi''(\omega,T)$ for the noninteracting system shows a stronger frequency dependence. Similar differences between noninteracting and interacting ensembles have also been observed in recent experimental studies.[3,5,10,13]

Magnetic relaxation, and in particular the ageing phenomenon, provides a unique tool to reveal dynamics governed by correlations between the particles. In a typical ageing experiment the sample is cooled in zero field to the measurement temperature, where it is kept for a time t_w before applying the field. If correlations evolve during the wait time the magnetic relaxation will depend on the wait time; $\chi(t,t_w)$. This procedure is applicable also to our MC simulations. In Fig. 4(a) the magnetic relaxation is plotted for two different wait times, $t_w = 100$ mcs and 1000 mcs, for different concentrations at the temperature $T = 20$ K. In the dilute, noninteracting systems no dependence on t_w can be detected, while on increasing the concentration ageing appears. To further illustrate the differences it is useful to plot the relaxation rate, $S(t,t_w) = \partial\chi(t,t_w)/\partial \ln(t)$ as in Fig. 4(b). A wait time dependence is characteristic of collective spin-glass-like dynamics. It is seen from Fig. 4 that not only does the dipole-dipole interaction give rise to a pronounced ageing behavior, but the relaxation is altered on all time scales studied. For observation times much shorter than the relaxation time τ of the noninteracting system, the magnetization and the relaxation rate are higher for the concentrated systems than for the noninteracting system. This indicates that the dipole-dipole interaction lowers some of the energy barriers and enhances the flipping probabilities at times close to the microscopic flip time. At observation times of the order of τ the relaxation rate is substantially suppressed for the concentrated systems and hence the relaxation will prevail to logarithmically much longer times than for the noninteracting system.

The magnetic relaxation is strongly dependent on temperature, and the dependence differs significantly for interacting and noninteracting systems. In Fig. 5 the relaxation and relaxation rate are plotted for the concentrations 0.1 and 7% in the temperature interval 20 to 80 K. For the 7% sys-

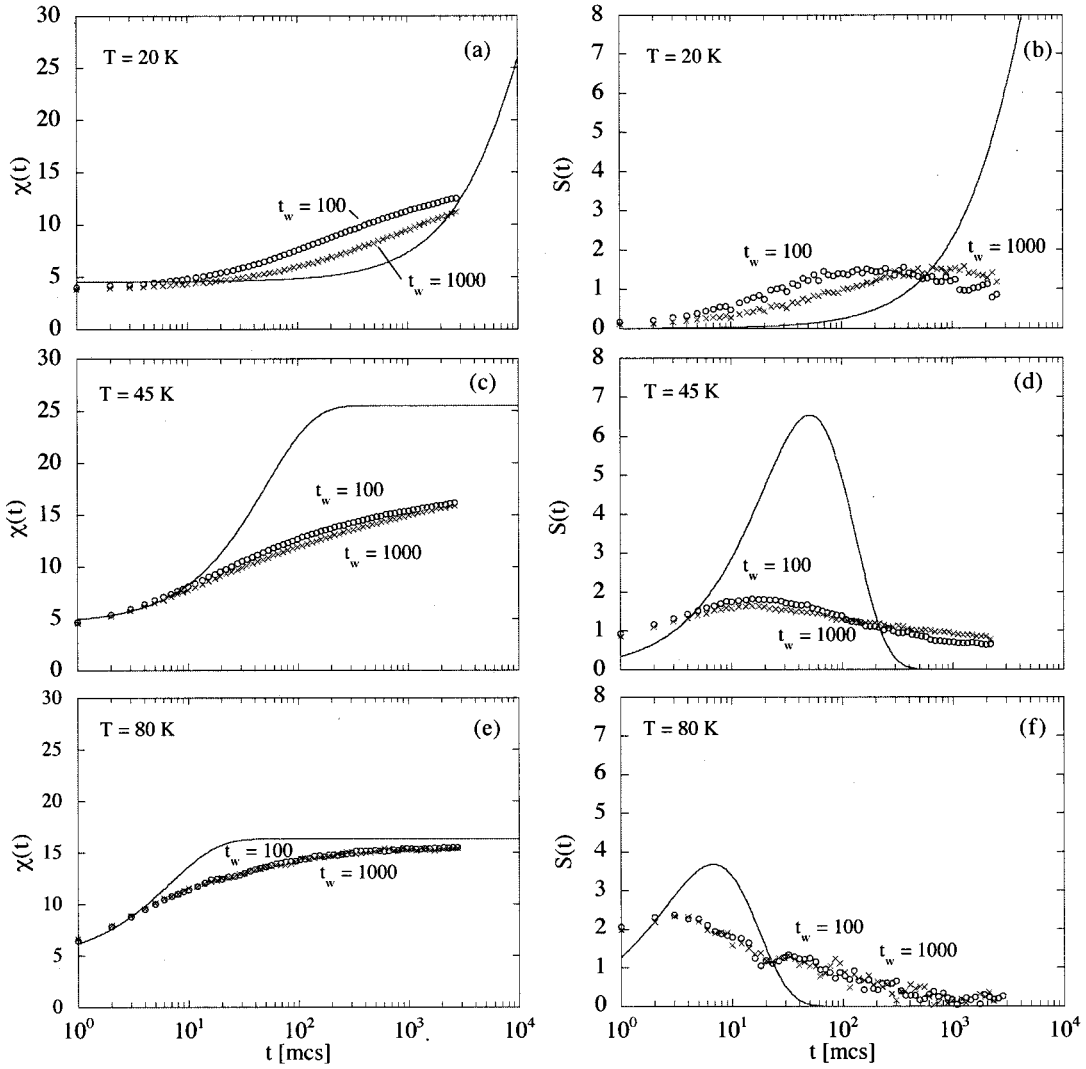

FIG. 5. ZFC susceptibility $\chi(t)$ and relaxation rate $S(t)=\partial\chi(t)/\partial\ln(t)$ for the concentrations $\epsilon=0.1$ and 7% at different temperatures. $t_w=100$ and 1000 mcs. $N_{\rm tr}=200$. (a) $\chi(t;T=20\ {\rm K})$ (b) $S(t;T=20\ {\rm K})$, (c) $\chi(t;T=45\ {\rm K})$, (d) $S(t;T=45\ {\rm K})$, (e) $\chi(t;T=80\ {\rm K})$, (f) $S(t;T=80\ {\rm K})$.

tem, the results using two different wait times, 100 and 1000 mcs, are plotted. On increasing the temperature it is observed that the wait time effect gradually vanishes. At $T=80$ K the magnetization almost reaches equilibrium in the time window of the simulation and consequently the relaxation rate approaches zero at long time.

An often studied quantity in simulations on random systems is the spin-spin autocorrelation function $q(t)$, here defined as $q(t)=\Sigma_i V_i^2\hat{\mu}_i(t+t_w)\cdot\hat{\mu}_i(t_w)/\Sigma_i V_i^2$. In Fig. 6 the autocorrelation function for the most concentrated system is plotted for different temperatures and two different wait times. A wait time effect is clearly observed, showing that the autocorrelation function $q(t;t_w)$ represents an alternative for investigating the ageing behavior in magnetic particle systems. $q(t)$ also has the advantage of being calculated in zero external field.

All results presented above have been obtained for monodispersive systems. On fabricating particles one always ends up with a distribution of particle sizes, often well described by a log-normal distribution. To check the influence of a size distribution, we have also studied ensembles where the particle sizes vary according to a log-normal distribution.[14] The main effect of the size distribution is to broaden the susceptibility maxima and the peaks are moved to higher temperatures as compared to the results shown in Fig. 3 for the monodispersive system. Still, the overall concentration dependence remains rather similar. Moreover, magnetic relaxation simulations showed that the ageing behavior also exists in the concentrated systems with a particle-size distribution.

IV. CONCLUSIONS

We have investigated dynamic magnetic properties of ensembles of monodispersive small magnetic particles of different concentrations using a relatively simple MC model. It is found that collective behavior to a large extent governs the dynamics at low temperatures in a concentrated system. The collective behavior of the concentrated system is manifested in the appearance of magnetic ageing and in a remarkable broadening of the relaxation function compared to the narrow Debye relaxation of a noninteracting system. The results show a qualitative agreement with corresponding experimen-

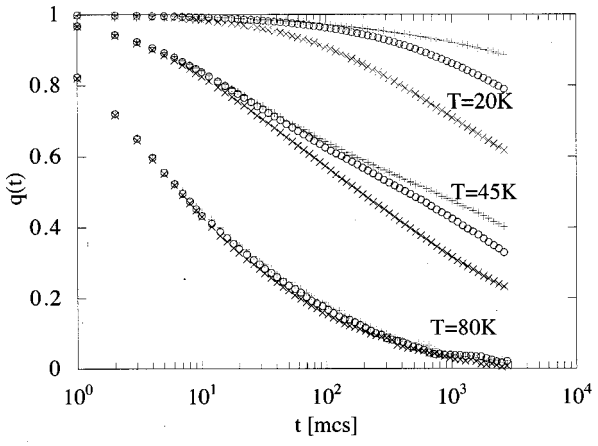

FIG. 6. The particle autocorrelation function, $q(t)=\Sigma_i V_i^2 \hat{\mu}_i(t+t_w)\cdot\hat{\mu}_i(t_w)/\Sigma_i V_i^2$ at different temperatures and wait times: $T=20$, 45, and 80 K and $t_w=100$, 1000, and 10 000 mcs. $\epsilon=7\%$, $N_{\rm tr}=200$.

tal results obtained from studies on interacting magnetic nanoparticle systems.[3,9,11,13]

ACKNOWLEDGMENT

Financial support from the Swedish Natural Science Research Council is gratefully acknowledged.

APPENDIX: NONINTERACTING PARTICLE ENSEMBLE

For the monodispersive noninteracting case, the calculations can be performed analytically. In the low-field limit, i.e., for small $x\equiv\mu_0 M_s H_a/K$, Eq. (2.4) yields to first order in x the minima $\alpha_1=x\,\sin(\psi)/2$ and $\alpha_2=\pi-x\,\sin(\psi)/2$ and the saddle point $\alpha_s=\pi/2+x\,\cos(\psi)/2$. The corresponding energies are $E_1=-KV[1+x\,\cos(\psi)]$, $E_2=-KV[1-x\,\cos(\psi)]$ and $E_s=-KVx\,\sin(\psi)$. The $\hat{z}$ component of the particle magnetizations are $m_1=M_s\,\cos(\psi-\alpha_1)\approx M_s[\cos(\psi)+x\,\sin^2(\psi)/2]$ and $m_2\approx M_s[-\cos(\psi)+x\,\sin^2(\psi)/2]$.

In an ensemble of independent particles, all with the same easy axis, with an angle ψ between the easy axis and the applied field, the fraction of magnetic moments in the m_1 direction is $n^+(t)=n_{\rm eq}+(0.5-n_{\rm eq})e^{-t/\tau}$, where $\tau=\tau_0/(e^{-\beta(E_s-E_1)}+e^{-\beta(E_s-E_2)})$ and $n_{\rm eq}=1/(1+e^{-\beta(E_2-E_1)})$. In the low-$x$ limit, $\tau\approx 0.5\tau_0 e^{\beta KV}$ and $n_{\rm eq}\approx\frac{1}{2}[1+\beta KVx\,\cos(\psi)]$. The ZFC magnetization is then given by

$$\begin{aligned} m(t)&=n^+(t)m_1+[1-n^+(t)]m_2 \\ &=M_s[(2n_{\rm eq}-1)(1-e^{-t/\tau})\cos(\psi)+x\,\sin^2(\psi)]. \end{aligned} \tag{A1}$$

Using the fact that $2n_{\rm eq}-1=\beta KVx\,\cos(\psi)$ and averaging over ψ in a system with random particle easy axes give

$$\chi(t)=\mu_0\frac{M_s^2}{3K}\left[1+\frac{KV}{k_BT}(1-e^{-t/\tau})\right]. \tag{A2}$$

The appearance of a nonzero value at $t=0$ is due to the fact that the locations of the minima change for the particle magnetic moments as soon as the field is applied at $t=0$

The ac susceptibility is given by

$$\begin{aligned} \chi(\omega)&=\int_0^\infty (d\chi/dt)e^{-i\omega t}dt \\ &=\int_0^\infty \mu_0\frac{M_s^2}{3K}\left[\delta(t)+\frac{KV}{k_BT}\frac{e^{-t/\tau}}{\tau}\right]e^{-i\omega t}dt \\ &=\mu_0\frac{M_s^2}{3K}\left[1+\frac{KV}{k_BT}\frac{1}{1+i\omega\tau}\right] \end{aligned} \tag{A3}$$

or

$$\chi'(\omega)=\mu_0\frac{M_s^2}{3K}\left[1+\frac{KV}{k_BT}\frac{1}{1+(\omega\tau)^2}\right], \tag{A4}$$

$$\chi''(\omega)=\mu_0\frac{M_s^2}{3}\frac{V}{k_BT}\frac{\omega\tau}{1+(\omega\tau)^2}. \tag{A5}$$

[1] L. Néel, Ann. Géophys. **5**, 99 (1949); W. F. Brown, Phys. Rev. **130**, 1677 (1963).

[2] Weili Luo, Sidney R. Nagel, T. F. Rosenbaum, and R. E. Rosensweig, Phys. Rev. Lett. **67**, 2721 (1991).

[3] T. Jonsson, J. Mattsson, C. Djurberg, F. A. Khan, P. Nordblad, and P. Svedlindh, Phys. Rev. Lett. **75**, 4138 (1995).

[4] C. Djurberg, T. Jonsson, P. Svedlindh, P. Nordblad, J. Z. Jiang, S. Mørup, H. Sang, S. Y. Zhang, and Y. W. Du, in *Magnetic Hysteresis in Novel Magnetic Materials*, edited by H. Hadjipanayis (Kluwer, Dordrecht, in press).

[5] E. Vincent, Y. Yuan, J. Hammann, H. Hurdequint, and F. Guevara, J. Magn. Magn. Mater. **161**, 209 (1996).

[6] *Monte Carlo Methods in Statistical Physics*, edited by K. Binder, Topics in Current Physics Vol. 7 (Springer-Verlag, Berlin, 1978).

[7] A. T. Ogielski, Phys. Rev. B **32**, 7384 (1985); J.-O. Andersson, J. Mattsson, and P. Svedlindh, *ibid.* **46**, 8297 (1992); J.-O. Andersson, J. Mattsson, and P. Svedlindh, *ibid.* **49**, 1120 (1994).

[8] R. W. Chantrell, G. N. Coverdale, M. El-Hilo, and K. O'Grady, J. Magn. Magn. Mater. **157**, 250 (1996).

[9] T. Jonsson, J. Mattsson, P. Nordblad, and P. Svedlindh, J. Magn. Magn. Mater. **168**, 259 (1997).

[10] J. L. Dormann, F. Dórzaio, F. Lucari, E. Tronc, P. Prené, J. P. Jolivet, D. Fiorani, R. Cherkaoui, and M. Nogués, Phys. Rev. B **53**, 14 291 (1996).

[11] A. Labarta, O. Iglesias, Ll. Balcells, and F. Badia, Phys. Rev. B **48**, 10 240 (1993).

[12] E. Vincent, J. Hammann, P. Prené, and E. Tronc, J. Phys. I **4**, 273 (1994).

[13] Jinlong Zhang, C. Boyd, and Weili Luo, Phys. Rev. Lett. **77**, 390 (1996).

[14] The log-normal distribution is given by $g(r)=(1/\sqrt{2\pi}\sigma r)\exp[-\ln^2(r/r_m)/(2\sigma^2)]$.